A Better Sunscreen: Structural Effects on Spectral Properties

Lawrence A. Huck and William J. Leigh*

Department of Chemistry and Chemical Biology, McMaster University, Hamilton ON, L8S 4M1, Canada

**leigh@mcmaster.ca*

Our recent restructuring of the second- and third-year chemistry undergraduate laboratory program involved the creation of a set of integrated laboratory courses to replace the individual laboratory components associated with our honors courses in analytical, inorganic, organic, and physical chemistry. The primary goal was to blur the customary divisions between the traditional chemistry subdisciplines and develop a multidisciplinary approach to laboratory teaching. One additional change that was viewed favorably by the students was the addition of *scenarios*, which provide a distinct, real-world focus for each experiment and helps to accentuate the links between the chemistry subdisciplines *(1)*. As we redesigned the course, we looked at several of our existing experiments to see how they could be adapted to fit the new model; one such experiment that seemed adaptable to the new model was the classic mixed-aldol synthesis of dibenzylideneacetone, **1**:

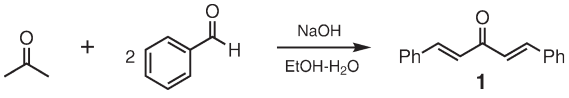

1 (1)

Variations of this aldol reaction have been discussed in this *Journal (2, 3)*. Both publications described the use of cyclic ketones and substituted benzaldehydes in place of acetone and benzaldehyde, respectively, and focused on methods to incorporate these into the synthetic experiment. With this as a starting point, we considered ways in which these modifications could best be fit into our new laboratory program.

Experimental Design

One property that makes **1** stand out from the products of many undergraduate organic syntheses is its bright yellow color and strong absorption in the UV-A region of the spectrum, an effect of the π-conjugation; it is for this reason that **1** has found use as a sunscreen *(4)*. Because the geometries of and degree of conjugation in cyclic analogues of **1** are different, so too are the UV−vis absorption characteristics *(5, 6)*. With this in mind, the following scenario was given to the students:

- We have been approached by a local group with an idea for a potential start-up company, whose main endeavor will be the manufacture of a new-and-improved sunscreen. One of the group is a chemist and has suggested that a suitable candidate might be obtained by modifying the structure of dibenzylideneacetone (DBA), a molecule used in some commercial sunscreens. In particular, the goal is to improve the absorption of ultraviolet radiation in the deleterious UV-A region (315−400 nm). DBA absorbs in this wavelength region because of its highly conjugated structure. The group believes it may be possible to improve the π-conjugation by preventing rotation of the σ bonds attached to the carbonyl carbon, thus, constraining the π bonds to lie in the same plane as the C═O group. The three proposed molecules are shown below (DBA-5, DBA-6, and DBA-7). We have been employed to test the feasibility of this idea and to explain the results.

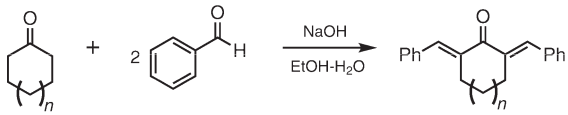

(2)

5, n = 0
6, n = 1
7, n = 2
8, n = 3

Students were organized into groups of four and asked to synthesize **1**, **5**, **6**, and **7** (eq 2) following a general procedure, each student in the group synthesizing a different molecule in the series. Reaction times are short (30−45 min) and conditions range from room temperature stirring (for **1**) to refluxing (for **5**−**7**). The products are isolated by vacuum filtration and are purified by recrystallization from methanol or methanol−chloroform. Recrystallized yields varied, but tended to be higher for **1** and **5** (∼70%) than for **6** and **7** (∼20%). Students record the ^{1}H NMR, IR, and UV spectra of the particular analogue they make and then tabulate the data within the group. The corresponding spectral data for **8** are provided to the students as well to broaden the comparison; we found the synthesis of this compound *(6−8)* to be more difficult than the others and inappropriate for a 4-h laboratory period. Once the synthesis and characterization is complete, the groups meet together with the instructor in a 60−90 min tutorial to compile their results and to discuss their interpretation.

Hazards

Acetone, ethanol, benzaldehyde, and the cycloketones are flammable. In addition, they may cause irritation to skin, eyes, and respiratory tract and may be harmful if swallowed or inhaled. Chloroform is a carcinogen, is toxic by inhalation, and can cause respiratory irritation. Sodium hydroxide is caustic; it causes burns to any area of contact. All work should be carried out in a fume hood. Goggles, gloves, and a lab coat should be worn.

Discussion

To understand the results of this experiment, knowledge of the geometries of the molecules is paramount. Although this presents a molecular modeling opportunity for the students,

10.1021/ed1004867 Published on Web 10/06/2010

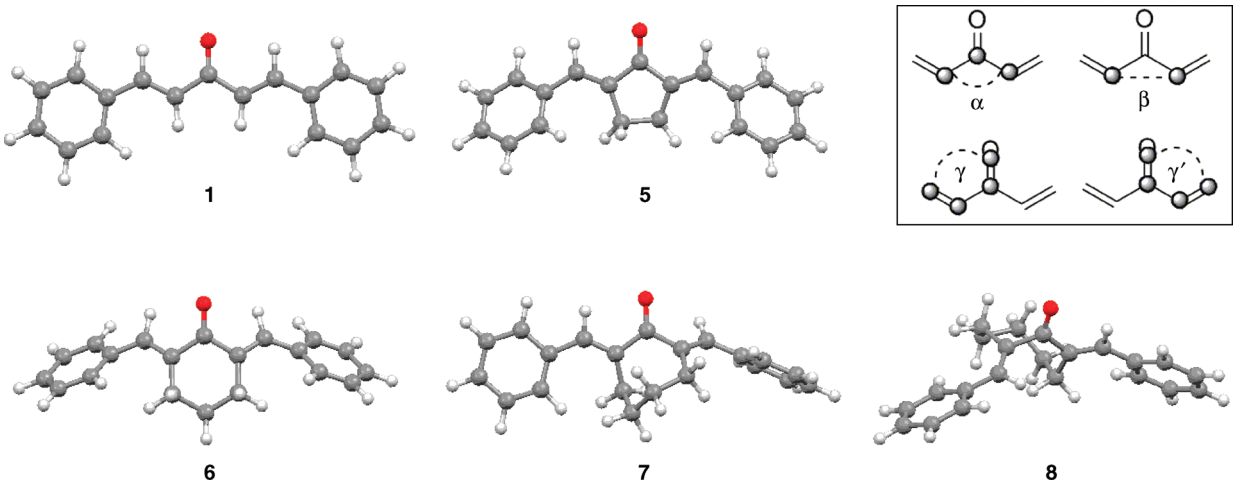

Figure 1. Ball-and-stick models of the geometry-optimized structures of **1**, **5**−**8** and a diagram showing the relevant bond angle (α), torsional angles (γ, γ') and distance (β) used in the analysis of the spectroscopic properties of **1**, **5**−**8**.

Table 1. Distances, Bond Angles, and Torsional Angles As Determined from the Geometry-Optimized Structures

Cpd	β/Å	α/deg	γ/deg	γ'/deg
1	2.50	115.5	1.4	−1.3
5	2.40	106.9	8.2	11.2
6	2.56	117.1	27.6	−27.6
7	2.56	116.5	−21.6	−52.8
8	2.58	118.0	19.5	−97.2

we opted to provide them with geometry-optimized structures *(9)* as .xyz files viewable with software such as Mercury (available free for Mac and PC) (Figure 1). Using these files, the students measure relevant bond angles and distances, such as those shown in Figure 1 and summarized in Table 1. It is stressed to the students that these models represent time-averaged minimum energy structures and that molecular motion occurs in solution.

Because the focus of this laboratory is UV−vis spectroscopy, we will not go into the details of the ^{1}H NMR, ^{13}C NMR, and IR spectra other than to summarize the results. Our primary use of the ^{1}H NMR spectra was to have the students verify that the spectrum is consistent with their target molecule. Each student was also required to analyze the ^{1}H NMR spectrum of **1**, to gain experience measuring and interpreting coupling constants and to show that the spectrum is consistent with the (*E*,*E*) isomer. The students were not required to obtain the ^{13}C NMR spectrum, but they were provided with the chemical shifts of the carbonyl carbons in the spectra of the five molecules (Table 2): the chemical shift moves to successively lower frequency from **8** through **1** because the increasing conjugation leads to better delocalization of electron density in the π bond, which in turn leads to increased shielding of the carbonyl carbon *(10)*. In the IR spectra (Table 2), ν(CO) is lower than that expected for a typical ketone because conjugation weakens the C═O bond. On the other hand, ring strain forces rehybridization of the carbonyl carbon because the angle is smaller than 120°; this imparts more p character to the carbon and strengthens the C═O bond *(11)*. Because **5** has the smallest angle α, ν(CO) for **5** occurs at the highest frequency.

Table 2. Summary of the ^{13}C NMR, IR, and UV−Visible Spectral Data

Cpd	λ_{max}/nm[a]	ε/(L mol^{-1} cm^{-1})[a]	ν(C═O)/cm^{-1} [b]	^{13}C═O/ppm[c]
1	332	35,500	1651	189.0
5	355	42,400	1691	196.5
6	330	33,600	1661	190.4
7	299	26,600	1672	199.6
8	293	23,000	1666	204.8

[a] Solvent is 95% ethanol. [b] KBr disc. [c] Solvent is $CDCl_3$ and peaks are referenced to the solvent at 77.16 ppm.

The energies of the lowest energy π,π^* UV transitions of **1**, **5**−**8** vary in the order: **8** > **7** > **6** > **1** > **5**. The trend **8** > **7** > **6** > **1** is explainable from the trends in the torsional angles (γ and γ'); **1** is nearly planar, whereas in **8**, one of the double bonds is nearly perpendicular to the carbonyl, providing the greatest disruption to the conjugation. To illustrate this effect further, the spectrum of **8** (λ_{max} = 293 nm) is compared to that of benzylideneacetone (**2**; λ_{max} = 285 nm) *(12)*, which is given to the students during the tutorial.

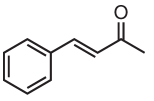

2

The trend in the spectra of the four dienones can be rationalized on the basis of the torsion angles measured from the computed geometry-optimized structures. Compound **5** exhibits the lowest energy transition despite torsion angles that are slightly greater than in **1**, and thus presents an apparent anomaly.

The frontier molecular orbitals, MOs, of **1** (which are given to the students) are shown in Figure 2. First, the students identify the MOs relevant to the observed UV transition (π_2,π_3^*) based on the magnitude of ε and briefly discuss why the latter is generally much larger than that of the n,π^* transition in the UV−vis spectra of aldehydes and ketones. The effects of solvent on the relative energies of n,π^* and π,π^* transitions are also briefly discussed; although it is the n,π^* absorption that is responsible for the yellow color of crystalline **1** and **5**−**8**, it is

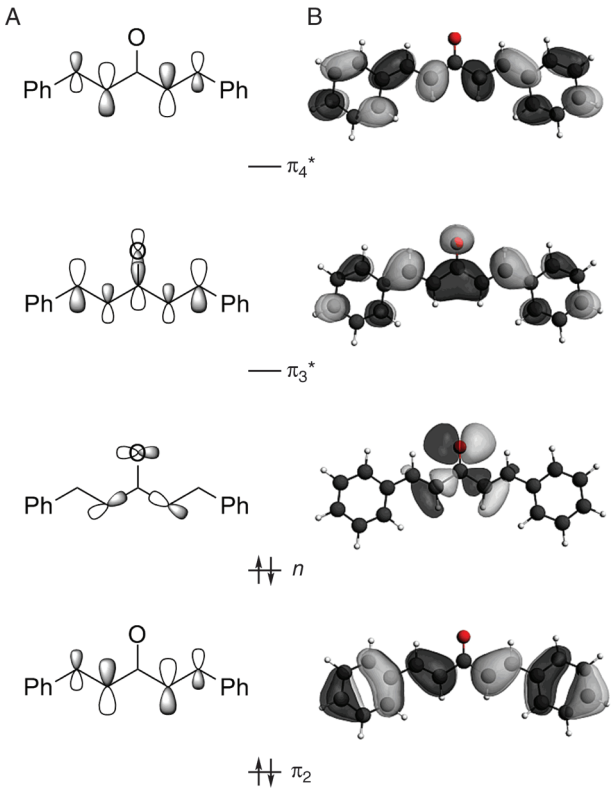

Figure 2. Frontier molecular orbitals of **1**: (A) simplified representation provided to the students for analysis and (B) pictorial representation as determined by DFT calculations *(11)*.

buried beneath the π,π^* band in the spectra they record (in 95% ethanol) owing to preferential stabilization of the *n* orbital by the hydrogen-bonding solvent *(13)*. Nevertheless, it is evident from the gradual fading of the color of the crystals, from bright yellow in **1** and **5** to colorless in **8**, that the energy of the n,π^* transition changes in a similar manner to the π_2,π_3^* transition.

Second, the students are asked to consider how the relative energies of π_2 and π_3^* must change to account for the lowest energy transition in the spectrum of **5** and they quickly point out that the energy of π_2 must increase or the energy of π_3^* must decrease. They are then asked to consider the differences in the geometries of **5** and **1** and what might cause the observed effect. There are two effects likely responsible for the energy difference. The first is ring strain induced by the contracted intra-annular bond angles associated with the three sp^2 carbons in the five-membered ring *(14)*; the students verify in the structure of **5** that the bond angles at the two carbons α to the carbonyl are contracted to a similar extent as that at the carbonyl carbon and that these are all significantly smaller than the corresponding angles in **1** and **6**. The strain raises the energy of the ground state (i.e., π_2) and excitation relieves this strain.

Third, the π_2 and π_3^* MOs are examined and the bonding and antibonding interactions between adjacent atoms identified. From their introduction to MO diagrams, students know that bonding interactions lower the energy and antibonding interactions raise the energy of a MO. Most students were surprised to learn that bonding and antibonding interactions between non-adjacent atoms can also affect MO energies. Compound **5** exhibits the smallest value of α and thus a shorter β distance than

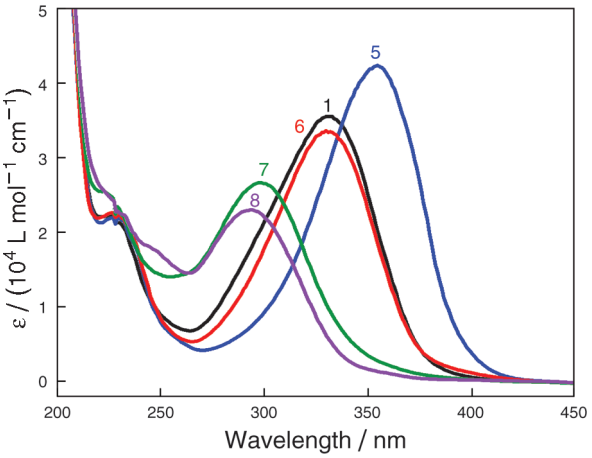

Figure 3. UV absorbance spectra of **1**, **5**, **6**, **7**, and **8** recorded in 95% ethanol.

in any of the other derivatives; this shortened distance may result in a slight increase in the energy of π_2 because of a through-space antibonding π-type interaction between the two carbons, whereas the energy of π_3^* is decreased slightly because of the through-space bonding interaction *(5)*. The effects of angle strain and enhanced conjugation give **5** the lowest π_2,π_3^* energy gap (and thus the longest wavelength absorption). The results are evident by overlaying the UV spectra of the five compounds (Figure 3). Not only does the UV spectrum of **5** provide the best coverage of the UVA region, it also has the largest value of ε and the lowest energy π,π^* transition. As a sunscreen, **5** would offer the best protection with the least amount of material.

Student Background

Students perform this laboratory in the second of the two level-II (second-year) honors chemistry integrated laboratory courses. To this point in time, students have gained considerable experience with preparative techniques in the laboratory. Students are also developing a familiarity with the interpretation of ^{1}H NMR and infrared spectra. The lecture courses have introduced molecular orbital theory and students can construct simple π-MO diagrams (ethylene, butadiene) and understand the corresponding electronic transitions. At this point in the program, we do not expect students at this level to reach all of the desired conclusions from this experiment (in regards to the underlying reasons for the spectroscopic trends in these molecules) independently. The laboratory manual contains enough detail for the best students to reach the desired conclusions (see the supporting information) on their own, but often only after the tutorial did the majority of the students fully appreciate the lessons afforded by the experiment. The experiment could be easily adapted for use in a more advanced laboratory course, where students could be expected to design the synthesis, carry out the computational study (for example), and explain the results with less leading by the instructor.

Acknowledgment

We thank McMaster's 2009 and 2010 Chemistry 2LB3 classes for their participation in this experiment.

Literature Cited

1. Lehman, J. W. *Operational Organic Chemistry: A Problem-Solving Approach to the Laboratory Course*, 3rd ed.; Prentice-Hall, Inc.: Upper Saddle River, NJ, 1999.
2. Hathaway, B. A. *J. Chem. Educ.* **1987**, *64*, 367.
3. Hull, L. A. *J. Chem. Educ.* **2001**, *78*, 226.
4. A number of patents exist wherein dibenzylideneacetone is used in the sunscreen lotion in combination with zinc dioxide or titanium dioxide. For example: Thaman, L. A.; Deckner, G. E.; Sottery, J. P. U.S. Patent 5,516,508, 1996.
5. Tsukerman, S. V.; Kutulya, L. A.; Lavrushin, V. F. *Zh. Obshch. Khim.* **1964**, *34*, 3597.
6. Farrell, P. G.; Read, B. A. *Can. J. Chem.* **1968**, *46*, 3685.
7. Ezzell, B. R.; Fluck, E. R.; Haefele, L. R. U.S. Patent 3,937,710, 1976.
8. Ali, M. I.; Hammam, A. E.-F. G.; Youssef, N. M. *J. Chem. Eng. Data* **1981**, *26*, 214.
9. *ADF2008.01d*, SCM, Theoretical Chemistry, Vrije Universiteit: Amsterdam, The Netherlands, http://www.scm.com (PW91-TZP) (accessed Sep 2010).
10. Breitmaier, E.; Voelter, W. *Carbon-13 NMR Spectroscopy: High-Resolution Methods and Applications in Organic Chemistry and Biochemistry*, 3rd ed.; VCH Publishers: New York, 1987; Ch 3.
11. Pavia, D. L.; Lampman, G. M.; Kriz, G. S. *Introduction to Spectroscopy*, 2nd ed.; Harcourt Brace College Publishers: New York, 1996; pp 38, 58.
12. Sadtler Standard Spectra Indices, Sadtler Research Laboratories Ltd.: Philadelphia, **1988**. UV 40379.
13. Connors, R. E.; Ucak-Astarlioglu, M. G. *J. Phys. Chem. A.* **2003**, *107*, 7684.
14. Schubert, W. M.; Sweeney, W. A. *J. Am. Chem. Soc.* **1955**, *77*, 2297.

Supporting Information Available

Laboratory handout for the students; instructor notes; geometry-optimized .xyz files with viewing instructions; and ^{1}H and ^{13}C NMR spectral data. This material is available via the Internet at http://pubs.acs.org.

